

## Overview

The **Bolometric Bond Albedo** is the albedo that represents the total reflected radiation from the asteroid, at all wavelengths, in all directions. We will derive an estimate of the Bolometric Bond Albedo for each OVIRS spot on Bennu using OVIRS calibrated spectral radiance factor and the global average best fit photometric model. The Bolometric Bond albedo requires two integrals: first, integrate the normalized disk-integrated brightness over phase angle for each wavelength, then integrate over wavelength.

1. Start with the global average **Radiance Factor** (RADF, or I/F) spectro-photometric model for Bennu at each wavelength. These functions are the output of the Photometric Modeling process. The best fit model will be either a Lommel-Seeliger model, a ROLO model, or a Minnaert Model. Note that the Lommel-Seeliger model used here contains a phase function in the form of an exponential function with a third order polynomial as the power, and the Minnaert model has 10-based exponential with a third order polynomial as the power.

2. Now create a map of OVIRS RADF (I/F) spectra photometrically corrected to zero phase angle, incidence = emission, or (e,e,0). This is called **Normal Albedo**. For Bennu and other dark surfaces the **Normal Albedo** value is close to the **Geometric Albedo** value because the effects of multiple scattering do not become significant until normal albedo (or normal reflectance) rises above 0.6 (Blackburn et al. 2010; Buratti 1984; Buratti and Veverka 1985). Hence, the **Normal Albedo** ( $A_{norm}$ ) will be assumed to be a good approximation of the **Geometric Albedo** ( $A_{geom}$ ) Map of Bennu.

3. Using the photometric model for Bennu at each OVIRS wavelength, calculate the **Phase Integral** at each wavelength (phase integral spectrum): First normalize each phase curve (at each wavelength  $k$ ) to be 1.0 at zero degrees phase angle - these are the  $\Phi(\alpha)$  functions. Use the equation:

$$q[k] = 2 * \text{Integral of } [\Phi(\alpha) * \sin(\alpha) d\alpha, 0 \text{ to } \pi]$$

( $k$  = wavelength, and for OVIRS it ranges over 1400 channels)

and integrate over all phase angles,  $\alpha$ , to get the Phase Integral "q". For the three models (LS, ROLO, and Minnaert),  $\Phi(\alpha)$  is the normalized disk-integrated brightness, defined in Blackburn et al. as:

$$\Phi(\alpha) = [f(\alpha)/f(0_0)] * [1 - \sin(\alpha/2) * \tan(\alpha/2) * \ln(\cot(\alpha/4))]$$

**Note:** Although this  $\Phi(\alpha)$  was originally derived for LS and ROLO models, our tests show that it can also be used for the Minnaert model.

3. Next, obtain **Spherical Albedo** ( $A_{sph}$ ), at each wavelength at each OVIRS spot, by multiplying the spot **Normal Albedo** from Step 2 above, by the appropriate **Phase Integral** value,  $q$ .

$$A_{sph}(k) = A_{norm}(k) * q(k)$$

4. Finally, calculate the **Bolometric Bond** albedo for each OVIRS spot by integrating the **Spherical Albedo** ( $A_{sph}$ ) over all wavelengths,  $k$ , from 0.4 to 4 microns (ideally from zero to infinity) (according to the equations in the "Reflectance and Albedo Quantities" document below), weighted by the solar spectral radiance (flux) model.

## Solar Flux Model

The approved solar flux model is given here:

The document below describes **what we did to generate the mission Solar Flux Model**. This is written by Mike Nolan, edited by Beth Clark. This information is also contained in the SAWG SIS: (PDF BELOW)

The **README file below** provides a description of the thinking behind the solar flux model sampling at OVIRS resolution by Dr. Mike Nolan:

2015 03 02  
OSIRIS-REx

Mike Nolan made an interpolated Solar spectrum spectral energy density model:

### -----README

Dennis Reuter suggests using Rieke 2008 (R08) as the reference solar spectrum. It was designed for a very similar purpose to what we want, generating an air-free solar spectrum for referencing spacecraft spectrometers and thermal modeling. Reading the paper, it has a quite detailed discussion of what is needed. There were several other spectra suggested. Several of them were the work of Thuillier et al (2002, 2003, 2004), but those only go out to 2.4 microns, shorter than the OVIRS cutoff. The others were mostly based on older data, and are discussed by Thuillier et al.

We noticed that the sample spacing of the R08 spectrum in the visible is lower than the resolution of the OVIRS instrumentation suite. Looking into the details of R08. It turns out to be a combination of several spectra from different instruments. In the range from 200 to 2400 nm, the spectrum used is that of Thuillier 2003, resampled to a lower resolution. We considered whether we could use the full-resolution spectrum for that part of the spectral range.

Resampling all of the spectra I had to a common high resolution (just a spline fit to a resolution of 0.01 nm, higher than any of the input spectra), the ratio of the various of Thuillier spectra to R08 is a noisy flat line. That is, it appears to have the same large-scale shape and integral as R08, but with finer structure. The Thuillier et al 2003 T03 paper instructs the reader to contact the author for the data, so I did that. The author recommended instead using the updated spectra from Thuillier 2004 (T04). He provided two spectra, one for "solar max" and one for "solar min", differing only shortward of 0.41 microns. As the encounter will occur nearer solar minimum, I used that one, but the difference is very small and over an almost negligible portion of the OVIRS range.

According to T04, they used a different solar constant than in earlier work, 1.4% higher. Plotting the ratio of T04/R08, that difference is clearly visible. T04 states that this is within the uncertainty of 2-4% for the various spectra.

To make a composite spectrum, I divided the spectrum from T04 by 1.014d0 and rescaled the axis units to those of R08. I then concatenated the portion of the T04 spectrum longward of 0.2 microns with the portion of the R08 spectrum longer than 2.398 microns.

The result is a spectrum that is everywhere higher resolution than the OVIRS instrumentation (perhaps by quite a bit too much over most of the spectrum). It has the solar constant of R08, but the spectral shape and sampling of T04.

2015 02 26

I rescaled again by a small factor (0.2 %) to make the integral (on the whole hi-res spectrum) come out to 1367 exactly.

I convolved the spectrum with a Gaussian to the approximate OVIRS resolution and then resampled at 2-nm spacing from 0.39 to 2.4 microns and 5 nm spacing from 2.4 - 4.37 microns. There are a few places where this spacing doesn't quite double-sample (from about 0.4 to 0.5 and 2.4 to 2.5 microns). The Gaussian FWHM was taken from an estimate from Dennis Reuter (see below). The Gaussian width was linearly interpolated and/or extrapolated in wavelength space using the given points and the cutpoints for the ~linear strip regions at 1100, 1800, and 2900 nm.

Error bars are from T04, 3% from 0.4 to 2.4 microns, and from R08, 2% above 2.4 microns.

The four columns in the list are wavelength (microns), spectral energy density ( $\text{W m}^{-2} \text{nm}^{-1}$ ), uncertainty ( $\text{W m}^{-2} \text{nm}^{-1}$ , assumed to be the absolute uncertainty reported for the underlying high-res spectrum), and smoothing resolution ( $\lambda / \Delta \lambda$  FWHM). I'm not sure whether the last column is useful or not.

This may need to be redone once we get the OVIRS as-built wavelength calibration, but it should already be pretty good.

2015 03 03

The definition of "Solar constant" isn't spelled out in the papers, but it's intended to be at 1 AU above the Earth's atmosphere. The exact value varies among authors, usually +/- 2 in the last digit, but with a recent value as different as 1361. I adopted  $1367 \text{ W/m}^2$  as a nominal value. At that level you just scale to what you want. Yes, you need to correct for  $1/r^2$  for Bennu.

The idea is that the OVIRS fluxes will be interpolated to the \*same\* scale, and that the scale is oversampled by ~2, so all you need to do is linearly interpolate if you need to tweak things. The values are per nm, not per bin, so if you rebin gently you don't have to integrate. If you rebin a lot you do, as you'll be averaging out the absorption lines. The raw OVIRS spectrum is more complicated, and Amy Simon-Miller's description of what's needed to get from there to the sampled spectrum involved some less-than-polite words suggesting that it's non-trivial.

I used a Gaussian as the estimated filter bandpass, though that's probably not really right. I would guess that the real bandpass is both squarer in the middle and has wider tails.

We could distribute a higher-resolution version if people want to do the smoothing and interpolation themselves using the same base spectrum. There are also some later papers with yet more modern results, but I doubt that the practical differences will be meaningful.

The variations in the higher-res solar spectrum are real, not (in general) noise, so you have to do flux-conserving smoothing with the filter bandpass if the resolutions don't match; you can't just spline or resample. It should work to spline them both to a much higher resolution and do your averaging there.

R08 Rieke, G. H.; Blaylock, M.; Decin, L.; Engelbracht, C.; Ogle, P.; Avrett, E.; Carpenter, J.; Cutri, R. M.; Armus, L.; Gordon, K.; Gray, R. O.; Hinz, J.; Su, K.; Willmer, Christopher N. A. (2008). Absolute Physical Calibration in the Infrared. *Astron. J.* 135, 2245-2263. DOI:dx.doi.org/10.1088/0004-6256/135/6/2245

R08 spectrum obtained from [http://iopscience.iop.org/1538-3881/135/6/2245/fulltext/aj271287\\_mrt7.txt](http://iopscience.iop.org/1538-3881/135/6/2245/fulltext/aj271287_mrt7.txt)

T03 Thuillier, G.; Hersé, M.; Labs, D.; Foujols, T.; Peetermans, W.; Gillotay, D.; Simon, P. C.; Mandel, H. (2003). The Solar Spectral Irradiance from 200 to 2400 nm as Measured by the SOLSPEC Spectrometer from the Atlas and Eureka Missions. *Solar Physics*, 214:1-22. DOI: dx.doi.org/10.1023/A:1024048429145

T04 Thuillier, G., F. Linton, T. N. Woods, R. Cebula, E. Hilsenrath, M. Hersé, and D. Labs 2004. Solar Irradiance Reference Spectra. In *Solar Variability and its Effect on Climate*, AGU monograph 141, eds J. Pap and P. Fox, p. 171. DOI: dx.doi.org/10.1029/141GM13

T04 spectrum provided by the author

Dr. Michael C. Nolan  
+1 787 878 2612x334 Fax: +1 787 878 1861 nolan@naic.edu  
Arecibo Observatory, HC 3 Box 53995, Arecibo, Puerto Rico 00612 USA

---

Resolution estimate from Dennis Reuter 2015 March 2.

All

The resolution vs. wavelength (both in nm) is fairly well represented by:

wavelength      full width at half maximum intensity

400                      2.1

600                      4.3

800                      5.7

1000                    7.5

1200                    7.5

1500                    8.3

1800                    10

2000                    8.5

2400                    10

2800                    11.7

2900                    7.8

3200                    8.7

3500                    9.5

3800                    10.3

4100                    11.1

4300                    11.6

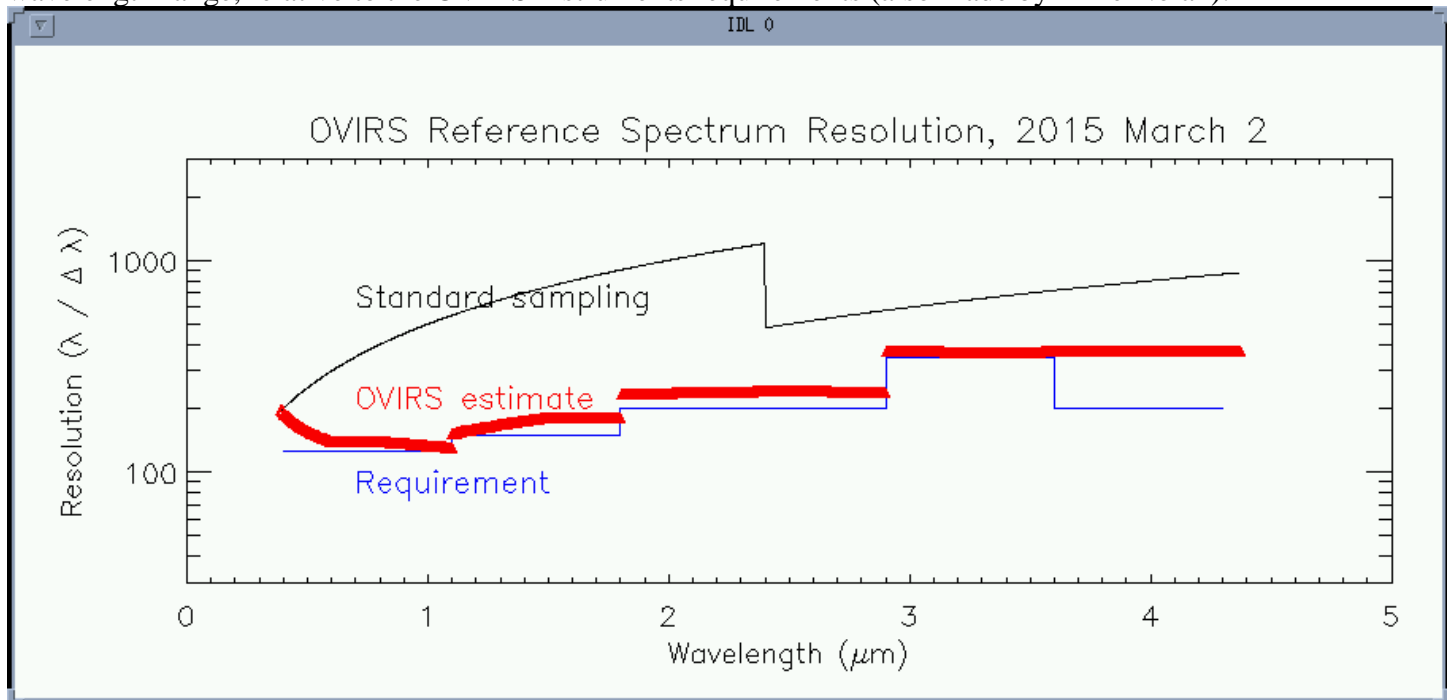
The sampling of every 2 nm from 400 to 2400 and 5 nm from 2400 to 4300 is a simplified representation of what will actually occur in the spectrometer. That is, the spectrum from 400 to 2400 will be measured using ~ 900 pixels (sometimes spaced less than 2 nm apart, sometimes greater than 2 nm apart) and the spectrum from 2400 to 4300 will be measured using ~ 380 pixels (sometimes spaced less than 5 nm apart, sometimes greater than 5 nm apart).

Please remember that for the actual data each spectral sample will be associated with its correct wavelength, which might vary a bit as a function of temperature and some other parameters. The purpose of the simplified spectral scale is just so that direct comparisons can be made quickly among various site selection map products. The actual spectra will always be available for more detailed science studies.

Thanks

Dennis

The graphic below illustrates how the spectral resolution changes with wavelength across the OVIRS wavelength range, relative to the OVIRS instruments requirements (also made by Mike Nolan):



## References

Blackburn et al. 2010. Solar Phase Curves and Phase Integrals for the Leading and Trailing Hemispheres of Iapetus from the Cassini Visual Infrared Mapping Spectrometer. *Icarus* 209, 738-744.

Blackburn, DG, Buratti, BJ, and Ulrich, R. 2011. A Bolometric Bond Albedo Map of Iapetus from Cassini VIMS and ISS and Voyager ISS. *Icarus* 212, 329-338.

Helfenstein et al. 1996. Galileo Photometry of Asteroid 243 Ida. *Icarus* 120, 48-65.

Howett, CJA, Spencer, JR, Pearl, J., and Segura, M. 2010. Thermal Inertia and Bolometric Bond Albedo Values for Mimas, Enceladus, Tethys, Dione, Rhea, Iapetus, as Derived from Cassini/CIRS Measurements. *Icarus* 206, 573-593.

Pitman, KM, Buratti, BJ, and Mosher, JA, 2010. Disk-integrated Bolometric Bond Albedos and Rotational Light Curves of Saturnian Satellites from Cassini VIMS. *Icarus* 206, 537-560.

Rieke, G. H.; Blaylock, M.; Decin, L.; Engelbracht, C.; Ogle, P.; Avrett, E.; Carpenter, J.; Cutri, R. M.; Armus, L.; Gordon, K.; Gray, R. O.; Hinz, J.; Su, K.; Willmer, Christopher N. A. (2008). Absolute Physical Calibration in the Infrared. *Astron. J.* 135, 2245-2263. DOI:dx.doi.org/10.1088/0004-6256/135/6/2245

R08 spectrum obtained from [http://iopscience.iop.org/1538-3881/135/6/2245/fulltext/aj271287\\_mrt7.txt](http://iopscience.iop.org/1538-3881/135/6/2245/fulltext/aj271287_mrt7.txt)

Thuillier, G.; Hersé, M.; Labs, D.; Foujols, T.; Peetermans, W.; Gillotay, D.; Simon, P. C.; Mandel, H. (2003). The Solar Spectral Irradiance from 200 to 2400 nm as Measured by the SOLSPEC Spectrometer

from the Atlas and Eureka Missions. Solar Physics, 214:1-22. DOI: [dx.doi.org/10.1023/A:1024048429145](https://doi.org/10.1023/A:1024048429145)

Thuillier, G., F. Linton, T. N. Woods, R. Cebula, E. Hilsenrath, M. Hersé, and D. Labs 2004. Solar Irradiance Reference Spectra. In Solar Variability and its Effect on Cl

For more information about Bond Albedo, please see the following "cheat sheet" - called the "Reflectance and Albedo Quantities" document:

**[Reflectance and Albedo Document \(V30\):](#)**

OrexSolarOVIRS.2015\_03\_02

By Mike Nolan

University of Arizona

To make a composite spectrum, I divided the spectrum from Thuillier et al. 2004 by 1.01400000 and rescaled the axis units to those of Rieke 2008. I then concatenated the portion of the Thuillier et al. 2004 spectrum longward of 0.2 microns with the portion of the Rieke 2008 spectrum longer than 2.398 microns.

The result is a spectrum that is everywhere higher resolution than the OVIRS instrumentation (perhaps by quite a bit too much over most of the spectrum). It has the solar constant of Rieke 2008, but the spectral shape and sampling of Thuillier et al. 2004. I rescaled by a small factor (0.2 %) to make the solar constant (integral over the whole hi-res spectrum) come out to 1367 exactly (to simplify – because the solar constant varies from year to year by one part in a thousand).

(Note: The definition of "solar constant" is not spelled out in the literature, but it's intended to be at 1 AU above the Earth's atmosphere. The exact value varies among authors, usually +/- 2 in the last digit, but with a recent value as different as 1361. I adopted 1367 W/m<sup>2</sup> as a nominal value. When the Solar Flux model is used, it must be scaled for distance (proportional to 1/r<sup>2</sup>.)

I then convolved the spectrum with a Gaussian to the approximate OVIRS resolution and then resampled at 2-nm spacing from 0.39 to 2.4 microns and 5 nm spacing from 2.4 - 4.37 microns. There are a few places where this spacing doesn't quite double-sample (from about 0.4 to 0.5 and 2.4 to 2.5 microns). The Gaussian FWHM was taken from an estimate from Dennis Reuter. The Gaussian width was linearly interpolated and/or extrapolated in wavelength space using the given sampling and the start and end points for the ~linear strip regions at 1100, 1800, and 2900 nm.

Error bars are from Thuillier et al. 2004, 3% from 0.4 to 2.4 microns, and from Rieke 2008, 2% above 2.4 microns.

The four columns in the data file "OrexSolarOVIRS.2015\_03\_02.txt" are wavelength (microns), spectral energy density (W m<sup>-2</sup> nm<sup>-1</sup>), uncertainty (W m<sup>-2</sup> nm<sup>-1</sup>, assumed to be the absolute uncertainty reported for the underlying high-res spectrum), and smoothing resolution ( $\lambda / \Delta \lambda$  FWHM).

Rieke, G. H.; Blaylock, M.; Decin, L.; Engelbracht, C.; Ogle, P.; Avrett, E.; Carpenter, J.; Cutri, R. M.; Armus, L.; Gordon, K.; Gray, R. O.; Hinz, J.; Su, K.; Willmer, Christopher N. A. (2008). Absolute Physical Calibration in the Infrared. *Astron. J.* 135, 2245-2263. DOI:[dx.doi.org/10.1088/0004-6256/135/6/2245](http://dx.doi.org/10.1088/0004-6256/135/6/2245) (spectrum obtained from [http://iopscience.iop.org/1538-3881/135/6/2245/fulltext/aj271287\\_mrt7.txt](http://iopscience.iop.org/1538-3881/135/6/2245/fulltext/aj271287_mrt7.txt))

Thuillier, G., F. Linton, T. N. Woods, R. Cebula, E. Hilsenrath, M. Hersé, and D. Labs 2004. Solar Irradiance Reference Spectra. In *Solar Variability and its Effect on Climate*, AGU monograph 141, eds J. Pap and P. Fox, p. 171. DOI: [dx.doi.org/10.1029/141GM13](http://dx.doi.org/10.1029/141GM13)

## BIDIRECTIONAL REFLECTANCE AND ALBEDO QUANTITIES

*Introduction: Most reflectance and albedo quantities are unitless quantities and are frequently misused or confused. Here, we review these quantities and summarize how viewing conditions vary for each quantity, relevant to OSIRIS-REx. Caution: our target asteroid is very dark, and multiple scattering is assumed to be relatively unimportant, but this assumption may not hold for brighter asteroids.*

### I. Bidirectional Reflectance Quantities

#### 1. Radiance Factor (RADF)

Hapke:

*Radiance Factor (RADF) is the **ratio** of the bidirectional reflectance of a surface **to** that of a perfectly diffuse surface illuminated at  $i = 0$  (the Sun!), rather than at the same angle of illumination.*

(Hapke 1993)

$$RADF(i, e, \alpha) = \pi r(i, e, \alpha),$$

where

$$r(i, e, \alpha) = \frac{\bar{\omega}_o}{4\pi} \frac{\mu_o}{\mu_o + \mu} \{ [1 + B(\alpha)] p(\alpha) + H(\mu_o)H(\mu) - 1 \} S(i, e, \alpha),$$

(The factor of  $\pi$  here is from the normalization and integration of the  $p(\alpha)$ ).

(Hapke 1993 eq. 8.89)

$\mu_o = \cos(i)$ ,  $\mu = \cos(e)$ ,  $i$  is the incidence angle (degrees),  $e$  is the emission angle (degrees),  $\bar{\omega}_o$  is the average particle single scattering albedo,  $1 + B(\alpha)$  is the opposition effect,  $p(\alpha)$  is the average particle single-scattering phase function,  $(H(\mu_o)H(\mu) - 1)$  describes the isotropic multiple scattering of light, and  $S(i, e, \alpha)$  is the macroscopic roughness.

Thus,

$$\begin{aligned} RADF(i, e, \alpha) &= \frac{\bar{\omega}_o}{4} \frac{\mu_o}{\mu_o + \mu} \{ [1 + B(\alpha)] p(\alpha) + H(\mu_o)H(\mu) - 1 \} S(i, e, \alpha) \\ &= \pi r(i, e, \alpha) = [I/\mathcal{F}](i, e, \alpha), \end{aligned}$$

$I$  is the radiance and has units of  $\text{W}/\text{m}^2/\text{nm}/\text{steradian}$ .  $J = \pi\mathcal{F}$  is the collimated light (irradiance) and has units of  $\text{W}/\text{m}^2/\text{nm}$ . Strictly speaking  $I/\mathcal{F}$  is a dimensionless quantity ( $\mathcal{F}$  has units of  $\text{W}/\text{m}^2/\text{nm}/\text{steradian}$  and  $\pi$  here has units of steradian).

(Hapke 1993)

*(RADF  $[I/\mathcal{F}]$  is what is measured by the spacecraft)*

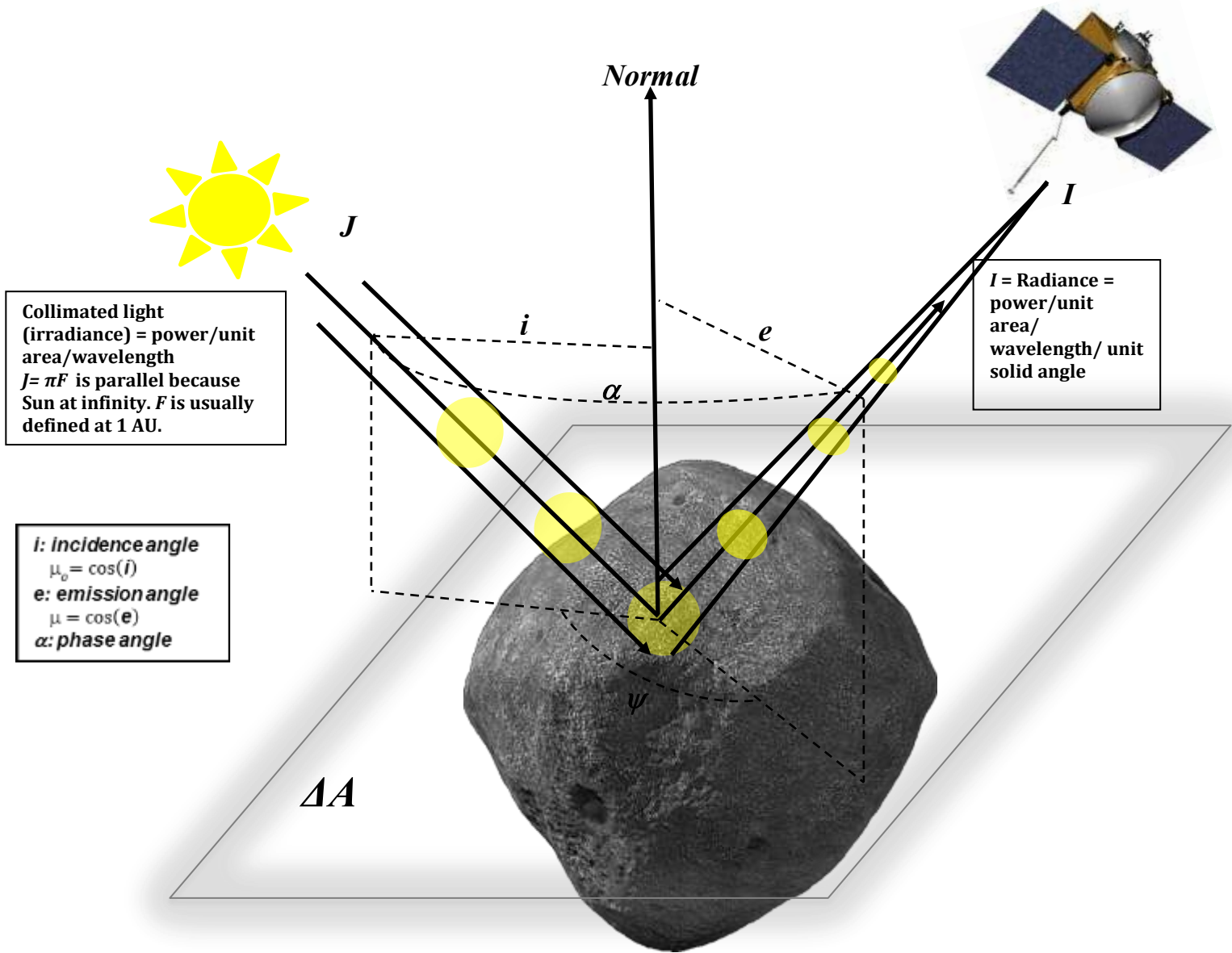


**Figure 1.** Schematic diagram of bidirectional reflectance from a surface element  $\Delta A$ , showing the various angles. The plane containing  $J$  and  $I$  is the scattering plane. If the scattering plane also contains  $N$ , it is called the principal plane.  $\psi$  is the azimuthal angle between the planes of incidence and emission [ $\cos(\alpha) = \cos(i)\cos(e) + \sin(i)\sin(e)\cos(\psi)$ .]  
 [Adopted from Hapke (1993)]

Lambert Model:

$$RADF(i, e, \alpha) = A_L \mu_o = [I/\mathcal{F}](i, e, \alpha),$$

where  $A_L$  is the Lambert albedo.

(Lambert 1759)

The Lambert model is a disk function that accounts only for limb darkening. However,  $A_L$  could be a function of phase angle ( $\alpha$ ).

Lambert Model with the Phase Function:

$$RADF(i, e, \alpha) = A_L f(\alpha) \mu_o = [I/\mathcal{F}](i, e, \alpha),$$

where  $f(\alpha) = 10^{-\frac{(\beta\alpha + \gamma\alpha^2 + \delta\alpha^3)}{2.5}}$  is a 3<sup>rd</sup> order polynomial phase function.

(d'Aubigny 2011)

This Lambert model accounts for limb darkening *and* the surface phase function.

Minnaert Model Disk Function:

$$RADF(i, e, \alpha) = \pi A_M \mu_o^k \mu^{k-1} = [I/\mathcal{F}](i, e, \alpha),$$

(Minnaert 1941)

where  $A_M$  and  $k$  are model parameters that characterize the Minnaert albedo and limb-darkening behavior of the surface, respectively.

The Minnaert disk function accounts only for limb darkening. However, both  $\pi A_M$  and  $k$  could be functions of phase angle ( $\alpha$ ).

Minnaert Model with the Phase Function:

$$RADF(i, e, \alpha) = \pi A_M f(\alpha) \mu_o^{k(\alpha)} \mu^{k(\alpha)-1} = [I/\mathcal{F}](i, e, \alpha),$$

where  $f(\alpha) = 10^{-\beta\alpha/2.5}$ ,  $\beta$  is the phase slope, and  $k(\alpha) = k_o + b\alpha$  characterizes the limb-darkening behavior of the surface and  $b$  captures the linear relationship between  $k$  and phase angle ( $\alpha$ ).  $k_o$  is the value of  $k$  at zero degrees phase angle.

(Li et al. 2009)

Or

$$f(\alpha) = 10^{-\frac{(\beta\alpha + \gamma\alpha^2 + \delta\alpha^3)}{2.5}}$$

(d'Aubigny 2011)

This Minnaert model includes the effects of limb darkening *and* the surface phase function.

*Note:* when  $i = 0$   $\mu_o \rightarrow 1$  and  $e = 0$   $\mu \rightarrow 1$ ,  $RADF(0,0,0) = \pi A_M f(\alpha)$ , which is consistent with normal reflectance when  $f(\alpha)$  is normalized to 1 at  $\alpha = 0$ .

Lommel-Seeliger Disk Function:

$$RADF(i, e, \alpha) = \frac{\bar{\omega}_o}{4} \frac{\mu_o}{\mu_o + \mu} = [I/\mathcal{F}](i, e, \alpha),$$

(Seeliger 1884)

where  $\bar{\omega}_o$  is the average particle single scattering albedo and  $f(\alpha)$  is an arbitrary function that describes the variation in surface reflectance with phase angle.

The Lommel-Seeliger disk function accounts only for limb darkening. However,  $\bar{\omega}_o$  could be a function of phase angle( $\alpha$ ).

Lommel-Seeliger Model with the Phase Function:

$$RADF(i, e, \alpha) = \frac{\bar{\omega}_o}{4} \frac{\mu_o}{\mu_o + \mu} f(\alpha) = [I/\mathcal{F}](i, e, \alpha),$$

(Helfenstein and Veverka 1989)

where  $f(\alpha)$  is an arbitrary function that describes the variation in surface reflectance with phase angle ( $\alpha$ ), and  $A_{LS} = \frac{\bar{\omega}_o}{4\pi}$  is Lommel-Seeliger albedo.

$$f(\alpha) = e^{\beta\alpha + \gamma\alpha^2 + \delta\alpha^3}$$

This Lommel-Seeliger/Veverka model includes the effects of limb darkening *and* the surface phase function.

ROLO Model:

$$RADF(i, e, \alpha) = \underbrace{\frac{\mu_o}{\mu_o + \mu}}_{\text{Describes limb darkening}} f(\alpha) = [I/\mathcal{F}](i, e, \alpha),$$

Describes limb darkening ←

Where  $f(\alpha) = \underbrace{C_0 e^{-C_1 \alpha}}_{\text{Describes opposition surge}} + \underbrace{A_0 + A_1 \alpha + A_2 \alpha^2 + A_3 \alpha^3 + A_4 \alpha^4}_{\text{4th order polynomial that describes phase function}}.$  (Buratti et al. 2011)

Describes opposition surge ←

→ 4<sup>th</sup> order polynomial that describes phase function

The ROLO model includes the effects of limb darkening *and* the surface phase function.

(These are the RADFs we will use to model Bennu's surface)

## 2. Reflectance Factor (REFF)

*Reflectance Factor (or reflectance coefficient) (REFF) is the **ratio** of the reflectance of the surface **to** that of a perfectly diffuse (Lambert) surface under the same conditions of illumination.*

(Hapke 1993)

$$REFF(i, e, \alpha) = \frac{r(i, e, \alpha)}{\frac{\mu_o}{\pi}} = \frac{\pi r(i, e, \alpha)}{\mu_o},$$

Thus

$$REFF(i, e, \alpha) = \frac{\bar{\omega}_o}{4} \frac{1}{\mu_o + \mu} \{ [1 + B(\alpha)] p(\alpha) + H(\mu_o)H(\mu) - 1 \} S(i, e, \alpha) = \frac{[I/\mathcal{F}](i, e, \alpha)}{\mu_o}$$

(This reflectance quantity is what is measured in the laboratory. For OVIRS spectral indices, the OVIRS data will be in these units.)

$$REFF(i=0, e=0, \alpha=0) = \frac{I/\mathcal{F}(i=0, e=0, \alpha=0)}{\mu_o} = \text{Normal Reflectance.}$$

(This is the most reasonable quantity to use when mapping the “albedo” of the surface.)

## 3. Hapke Bidirectional Reflectance Distribution Function (BRDF)

*Bidirectional Reflectance Distribution Function (BRDF) is the **ratio** of the radiance scattered by a surface into a given direction **to** the collimated power incident on a unit area of the surface.*

(Hapke 1993)

$$BRDF(i, e, \alpha) = \frac{Jr(i, e, \alpha)}{J\mu_o} = \frac{r(i, e, \alpha)}{\mu_o},$$

$J\mu_o$  is the incident radiant power per unit area of surface and  $Jr(i, e, \alpha)$  is the scattered radiance.

Thus

$$\begin{aligned} BRDF(i, e, \alpha) &= \frac{\bar{\omega}_o}{4\pi} \frac{1}{\mu_o + \mu} \{ [1 + B(\alpha)] p(\alpha) + H(\mu_o)H(\mu) - 1 \} S(i, e, \alpha) \\ &= [I/(\mu_o \pi \mathcal{F})](i, e, \alpha). \end{aligned}$$

(Functions of this form are requested by OSIRIS Instrument Teams to be used to predict Bennu’s brightness. See conclusion Table 2 showing relationship between RADF and BRDF.)

## II. Albedo Quantities

### 1. Lambertian Albedo

*Lambertian albedo* ( $A_L$ ) is the **ratio** of the total power scattered per unit area of a Lambert surface to the incident power per unit area.

(Hapke 1993)

$$A_L = \frac{P_L}{J\mu_o},$$

$P_L = \int_{2\pi} I(i, e, \alpha) \mu d\alpha = \int_{e=0}^{\pi/2} \int_{\alpha=0}^{2\pi} JK_L \cos i \cos e \sin e de d\alpha = \pi JK_L \mu_o$  is the total power scattered per unit area of Lambert surface into all directions of the upper hemisphere.

Where  $K_L = r_L(i, e, \alpha)/\mu_o$  is a constant (*Lambert's law*). When  $K_L$  is constant then we have a Lambertian surface.

Thus the *Lambert reflectance* is  $\pi r_L(i, e, \alpha) = A_L \mu_o = RADF(i, e, \alpha) = [I/\mathcal{F}](i, e, \alpha)$ .

Therefore

$$A_L = [I/(\mu_o \mathcal{F})](i, e, \alpha).$$

### 2. Geometric Albedo

*Physical albedo (a.k.a, Geometric albedo)* ( $A_{geo}$ ) is the **ratio** of the brightness of a body at zero phase angle  $\alpha = 0$  to the brightness of a perfect *Lambert disk* of the same radius and at the same distance as the body, but illuminated and observed perpendicularly.

(Hapke 1993)

$$A_{geo} = \int_{2\pi} r(e, e, 0) \mu d\Omega,$$

where  $d\Omega = 2\pi \sin(e) de = -2\pi d\mu$ .

Geometric Albedo is usually presented at one wavelength, the V passband, or  $0.55 \mu\text{m}$ .

#### 2.1 Lommel\_Seeliger

$$A_{geo} = \frac{A_{LS}}{2} \pi f(0) \int_0^{\pi/2} \cos(e) \sin(e) de = \frac{A_{LS}}{2} \pi f(0)$$

#### 2.2 ROLO

$$A_{geo} = f(0) \int_0^{\pi/2} \cos(e) \sin(e) de = \frac{f(0)}{2}$$

#### 2.3 Minnaert:

$$A_{geo} = 2\pi A_M f(0) \int_0^{\pi/2} [\cos(e)]^{2k_o} \sin(e) de = A_M \frac{2\pi}{2k+1} f(0)$$

$k_o$  is the value of  $k(\alpha)$  at zero degrees phase angle.

### 3. Normal Albedo

The *normal albedo*  $A_n$  is the ratio of the brightness of a surface observed at zero phase angle from an arbitrary direction to the brightness of a perfectly diffuse surface located at the same position, but illuminated and observed perpendicularly.



$$A_n = \frac{[Jr(e,e,0)]}{[\frac{J}{\pi}]} = \pi r(e, e, 0)$$

### 4. Spherical Bond Albedo

*Spherical bond albedo* (a.k.a., *Bond albedo*) ( $A_{sph}$ ) is the total fraction of incident irradiance at one wavelength (usually 0.55  $\mu\text{m}$ ) scattered by the body into all directions.

(Hapke 1993)



$$A_{sph} = \frac{1}{\pi} \int_{2\pi} \int_{2\pi} r(i, e, \alpha) \mu d\Omega_i d\Omega_e,$$

where  $d\Omega_i = \sin(i) di d\psi$  and  $d\Omega_e = \sin(e) de d\psi$  with  $\psi$  is the azimuth.

The *spherical bond* albedo can also be expressed as  $q A_{geo}$ , where  $q$  is the phase integral, defined as:

$$q = 2 \int_0^\pi \Phi(\alpha) \sin(\alpha) d\alpha$$

where  $\Phi(\alpha) \equiv \frac{F(\alpha)}{F(0^\circ)}$  is the disk-integrated brightness at phase angle  $\alpha$ , assuming a spherical body (Buratti and Veverka 1983).  $F(\alpha)$  is the phase dependence of the disk-integrated flux defined as:

$$F(\alpha) = \frac{R^2}{r^2} \int_{\alpha-\frac{\pi}{2}}^{\frac{\pi}{2}} \int_{\alpha-\frac{\pi}{2}}^{\frac{\pi}{2}} \frac{I}{F}(i, e, \alpha) \cos(w) \cos^2(\psi) dw d\psi,$$

where  $w$  = photometric longitude,  $\psi$  = photometric latitude,  $R$  = radius of the satellite, and  $r$  = observer-satellite distance.

(This is the albedo quantity shown in Table 1 that requires observations covering phase angles from  $0^\circ \rightarrow 180^\circ$ .)

#### 4. Bolometric Bond Albedo

*Bolometric bond albedo* ( $A_{bolo}$ ) is the average of the spherical *Bond albedo*  $A_{sph}(\lambda)$  weighted by spectral irradiance of the Sun  $J_S(\lambda)$ . This integrates *Spherical albedo* over all  $\lambda$ .

$$A_{bolo} = \frac{\int_0^{\infty} A_{sph}(\lambda) J_S(\lambda) d\lambda}{\int_0^{\infty} J_S(\lambda) d\lambda},$$

where  $J_S(\lambda)$  is the solar flux spectrum ( $\lambda$ ).

(The OSIRIS-REx Science Team has adopted the solar flux model of Reike et al. 2008)

(This is the quantity required for Yarkovsky and thermal inertia measurements for OSIRIS-REx)

### III. Examples of Reflectance and Albedo Quantities:

**Table 1a.** Comparison of reflectance and albedo quantities for different asteroids:

	Ceres <sup>0</sup>	Ida <sup>1</sup>	Eros <sup>2</sup>	Eros <sup>3</sup>	Dactyl <sup>1</sup>	Gaspra <sup>1</sup>	Mathilde <sup>4</sup>	Vesta <sup>5</sup>	Bennu <sup>6,7</sup>	Phobos <sup>8</sup>	Deimos <sup>8</sup>
Geometric Albedo	0.088	0.206	0.290	0.23	0.198	0.23	0.047	0.38±0.01	0.045	0.071	0.068
Spherical Bond Albedo	0.020	0.081	0.12	0.093	0.073	0.12	--	0.20±0.02	0.016	0.021	0.027
Normal Reflectance	--	0.207	--	--	0.198	0.23	0.047	--	--	0.071	0.068

<sup>0</sup>Li et al. (2006). <sup>1</sup>Helfenstein et al. 1994, <sup>2</sup>Domingue et al. 2002, <sup>3</sup>Li et al. 2004, <sup>4</sup>Clark et al. 1999, <sup>5</sup>Li et al. 2013, <sup>6</sup>Hergenrother et al. 2013. <sup>7</sup>Emery et al. (2014). The geometric albedo and normal reflectance values are for 0.55  $\mu$ m. Note that Helfenstein and Domingue do not seem to agree on the meaning of Bond albedo terms. <sup>8</sup>Simonelli et al. (1998) and Thomas et al. (1996).

**Table 1b.** Comparison of reflectance and albedo quantities for different comets:

	9P/Tempel 1 <sup>1</sup>	19P/Borrelly <sup>2</sup>	81P/Wild 2 <sup>3</sup>	28P/Neujmin 1 <sup>4</sup>	2P/Encke <sup>5</sup>
Geometric Albedo	0.059±0.009	0.080±0.020	0.059	0.026	0.047
Spherical Bond Albedo	0.014±0.002	0.018	0.0093	--	--

<sup>1</sup>Li et al. (2013).<sup>2</sup>Li et al. (2007).<sup>3</sup>Li et al. (2009).<sup>4</sup>Campins et al. (1987).<sup>5</sup>Fernandez et al. (2000)

#### IV. Conclusions

- The value of albedo measured with an integrating sphere (in the laboratory) can be comparable to the *spherical bond* albedo of a body covered with the same material (Barucci et al. 2012).
- The *bolometric bond* albedo is *not* equal to the *spherical bond* albedo. The bolometric albedo is the average of the spectral bond albedo weighted by spectral irradiance of the Sun.
- It is generally assumed that the *spherical bond* albedo in the V passband (~0.55  $\mu\text{m}$ ) is a good representation of the *bolometric bond* albedo. This is because (a) most of the Sun's energy is in the visible and (b) most spectra of Solar System bodies do not change drastically over the UV/Vis (Emery, personal communication).
- For disk-resolved observations and Lommel-Seeliger surfaces, the value of  $I/(\mu_o\mathcal{F})$  is close to the value of the *geometric* albedo at wavelength  $\lambda$  when observed at a phase angle  $\alpha = 0$ .  $I/\mathcal{F} = 1$  is for a flat *Lambertian* surface when viewed at normal incidence.
- For disk-integrated observations and Lommel-Seeliger surfaces, the *geometric* albedo, which is similar to the *normal* albedo, is a measure of a surface's brightness relative to a perfectly scattering Lambertian disk.
- The Lambert and Minnaert functions are disk functions with no dependence on phase angle and account only for limb darkening. However, the Hapke, Minnaert, the Lommel-Seeliger/Veverka, and ROLO functions include surface phase functions and limb darkening.
- For Bennu and other dark objects, the normal reflectance value is close to  $(1/\pi)$  times the geometric albedo value for Lommel-Seeliger surfaces. The normal reflectance is the most reasonable quantity to use when mapping the "albedo" of the surface.
- Lester et al. (1979), who called the normal albedo ( $p_n$ ), found that the geometric albedo ( $p$ ) is equivalent to the normal albedo ( $p_n$ ) for Lommel-Seeliger surfaces.
- **Table 2.** In this table we show various models converted from RADF to BRDF by division of  $\pi\mu_o$ . Note that in our equations,  $I/\mathcal{F}$  is unitless, where  $I$  = measured radiance from the surface in  $\text{W}/\text{m}^2/\text{sr}/\text{nm}$  and  $J = \pi\mathcal{F}$  = solar irradiance (flux) in  $\text{W}/\text{m}^2/\text{nm}$ .  $\pi$  has units of steradian and  $\mathcal{F}$  units of  $\text{W}/\text{m}^2/\text{nm}/\text{steradian}$ .

	<b>RADF</b>	<b>BRDF</b>
	$[I/\mathcal{F}](i, e, \alpha) =$	$\frac{[I/\mathcal{F}](i, e, \alpha)}{\pi\mu_o} =$
<i>Lambert Model</i>	$A_L f(\alpha)\mu_o$	$\frac{A_L f(\alpha)}{\pi}$
<i>Minnaert Model</i>	$\pi A_M f(\alpha)\mu_o^{k(\alpha)} \mu^{k(\alpha)-1}$	$A_M f(\alpha)\mu_o^{k(\alpha)-1} \mu^{k(\alpha)-1}$
<i>Lommel Seeliger Model</i>	$\frac{\bar{\omega}_o}{4} \frac{\mu_o}{\mu_o + \mu} f(\alpha)$	$\frac{\bar{\omega}_o}{4\pi} \frac{1}{\mu_o + \mu} f(\alpha)$
<i>ROLO Model</i>	$\frac{\mu_o}{\mu_o + \mu} f(\alpha)$	$\frac{1}{\pi} \frac{1}{\mu_o + \mu} f(\alpha)$

## References

- Barucci, M.A., Belskayaa, I.N., Fornasier, S., Fulchignoni, M., Clark, B.C., Coradini, C., Capaccioni, F., Dotto, E., Birlan, M., Leyrat, C., Sierks, H., Thomas, N., Vincenti, J.B. 2012. Overview of Lutetia's surface composition. *Planetary & Space Science* 66, 23-30.
- Blackburn, D.G., Buratti, B.J., Ulrich, R., Mosher, J.A. 2012. Solar phase curves and phase integrals for the leading and trailing hemispheres of Iapetus from the Cassini Visual Infrared Mapping Spectrometer. *Icarus* 209, 738-744.
- Buratti, J., Hicks, M.D., Nettles, J., Staid, M., Pieteres, C.M., Sunshine, J., Boardman, J., and Stone, T.C. 2012. A wavelength-dependent visible and infrared spectrophotometric function for the Moon based on ROLO data. *JGR* 116, E00G03.
- Campins, H., A'Hearn, M.F., McFadden, L.A., 1987. The bare nucleus of Comet Neujmin 1. *Astrophys. J.* 316, 847-857.
- Clark, B.E., Veverka, J., Helfenstein, P., Thomas, P. C.; Bell, J. F., Harch, A., Robinson, M. S., Murchie, S. L., McFadden, L. A., Chapman, C. R. 1999. NEAR Photometry of Asteroid 253 Mathilde. *Icarus* 140, 53-65.
- Clark, B.E., Binzel, R. P., Howell, E.S., Cloutis, E.A., Ockert-Bell, M., Christensen, P., Barucci, M.A., DeMeo, F., Lauretta, D.S.; Connolly, H., Soderberg, A., Hergenrother, C., Lim, L.; Emery, J., Mueller, M. 2011. Asteroid (101955) 1999 RQ36: Spectroscopy from 0.4 to 2.4  $\mu\text{m}$  and meteorite analogs. *Icarus* 216, 462-475.
- Domingue, D.L., Robinson, M., Carcich, B., Joseph, J., Thomas, P, Clark, B.E. 2002. Disk-integrated Photometry of 433 Eros. *Icarus* 155, 205-219.
- Drouet Aubigny, C. 2011. RQ36 Photometric Models and Their Implications for OCAMS. Draft V6.
- Fernández, Y.R., Lisse, C.M., Käufl, H.U., Peschke, Sibylle B., Weaver, H.A., A'Hearn, M.F., Lamy, P.L., Livengood, T.A., Kostiuk, T., 2000. Physical properties of the nucleus of Comet 2P/Encke. *Icarus* 147, 145-160.
- Hapke, B. 1993. *Theory of Reflectance and Emittance Spectroscopy*. Cambridge University Press.

- Hergenrother et al. 2013. The Design Reference Asteroid Document. OSIRIS-REx Mission.
- Helfenstein, P., Veverka, J., Thomas, P.C., Simonelli, D.P., Lee, P., Klaasen, K., Johnson, T.V., Breneman, H., Head, J.W., Murchie, S., Fanale, F., Robinson, M., Clark, B., Granahan, J., Garbeil, H., McEwen, A.S., Kirk, R.L., Davies, M., Neukum, G., Mottola, S., Wagner, R., Belton, M., Chapman, C., and Plicher, C. 1994. Galileo Photometry of Asteroid 951 Gaspra. *Icarus* 107, 37-60.
- Helfenstein and Veverka. 1989. Physical characterization of asteroid surfaces from photometric analysis. In *Asteroids II*. Univ. of Arizona Press, Tucson.
- Lambert, J.H., 1759. *L perspective affranchie de l'embaras du Plan geometral*. Zurich: Heidegger, 1759; VIII, 192 p. : 6 tavv.f.t. ; in 8.; DCC.16.29.
- Li, J.Y., A'Hearn, M.F., and McFadden, L.A. 2004. Photometric analysis of Eros from NEAR data. *Icarus* 172, 415-431.
- Li, J.Y., McFadden, L.A., Parker, J.W., Young, E.F., Thomas, P.C., Russell, C.T., Sykes, M.V., Stern, S.A., 2006. Photometric analysis of 1 Ceres and surface mapping from HST observations. *Icarus* 182, 143–160.
- Li, J.Y., A'Hearn, M.F., McFadden, L.A., Belton, M.J.S. 2007. *Icarus* 188, 195-211. *Icarus* 188 (2007) 195–211.
- Li, J.Y., A'Hearn, M.F., Farnham, T.L., McFadden, L.A., 2009. Photometric analysis of the nucleus of Comet 81P/Wild 2 from Stardust images. *Icarus* 204, 209-226.
- Li, J.Y., A'Hearn, M.F., Belton, M.J.S., Farnham, T., L., Klaasen, K.P., Sunshine, J.M., Thomas, P.C., Veverka, J. 2013. Photometry of the nucleus of Comet 9P/Tempel 1 from Stardust-NExT flyby and the implications. *Icarus* 222, 467-476.
- Minnaert, M. 1941. The Reciprocity Principle in Lunar Photometry. *Astrophys. J.* 93, 403–410.
- Rieke, G.H., Blaylock, M., Decin, L., Engelbracht, C., Ogle, P., Avrett, E., Carpenter, J., Cutri, R.M., Armus, L., Gordon, K., Gray, R.O., Hinz, J., Su, K., and Willmer, C.N.A. Absolute Physical Calibration in the Infrared. *The Astronomical Journal.* 135:2245-2263.
- Seeliger, H. 1884. Zur Photometrie des Saturnringses, *Astron. Nachr.*, 109, 305–314, doi:10.1002/asna.18841092002
- Simonelli, D., M. Wisz, A. Switala, D. Adinolfi, J. Veverka, P. C. Thomas, and P. Helfenstein 1998. Photometric properties of Phobos surface materials from Viking images. *Icarus* **131**, 52–77.
- Thomas, P. C., J. Veverka, J. F. Bell III, B. E. Clark, B. Carcich, J. Joseph, M. Robinson, L. A. McFadden, M. C. Malin, C. R. Chapman, W. Merline, and S. L. Murchie 1999. Mathilde: Size, shape and geology. *Icarus* **140**, 17–27.
- Takir, D., Clark, B.C., D'Aubigny, C.D., Hergenrother, C.W., Li, J.Y., Lauretta, D.S., and Binzel, R.P. Photometric models of disk-integrated observations of the OSIRIS-REx target Asteroid (101955) Bennu. Volume 252, Pages 393–399.